Improving EM Analysis for Sea Ice Thickness Estimation

Sandia National Laboratories is a multi-mission laboratory managed and operated by Sandia Corporation, a wholly Owned subsidiary of Lockheed Martin SAND2016-10608C for the U. S. Department of Energy's National Nuclear Security Administration under Contract DE-AC04-94AL85000

Cathleen A. Geiger[1], H. Allan Wienecke[2], Jesse P. Samluk[1], Chester J. Weiss[3,4]
[1]*University of Delaware, USA*
[2]*Independent Investigator, USA*
[3]*Sandia National Laboratories, Albuquerque, NM, USA*
[4] *University of New Mexico, Albuquerque, NM, USA*

Introduction

This project addresses a need within polar science communities to improve the interpretation of non-invasive, kilohertz (kHz) band electromagnetic (EM) observations of snow, ice, snow-ice, and sea ice. As a diagnostic tool, we employ a full-physics three-dimensional (3-D) electromagnetic model to advance understanding between surface EM measurements and subsurface composite structures. We are exploring and numerically optimizing novel EM sensor configurations to enable tech transfer for "next generation" EM instruments. The driving science question is: *Why is it so hard to match measurements between instruments with different footprint sizes?*

Motivational Model Outcomes

Spatial aliasing, scaling laws, and sensitivity of waveform/ filter shapes ignited our curiosity to re-examine fundamental assumptions in electromagnetic (EM) responses. Sensitivity of instrument-footprint width to geomaterial conductivity for uniform homogeneous layers are demonstrated below using our model - APhiD. Footprint area is not proportional to distance as traditionally postulated for homogeneous half-space solutions. Essentially, there is significant variation in instrument footprint even when an instrument remains at a constant height relative to the target area.

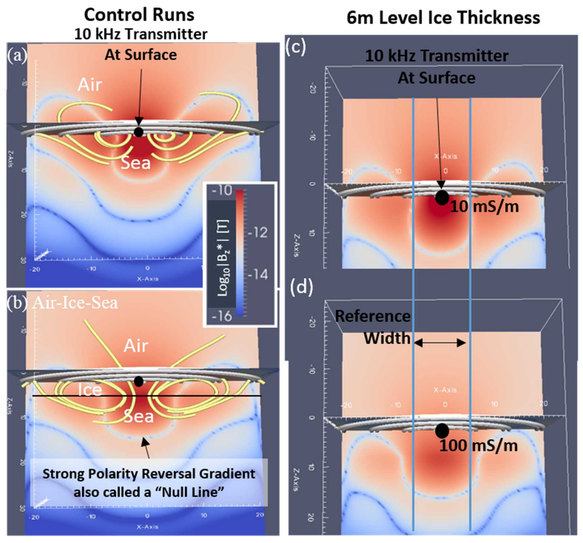

Figure 1. Sensitivity of instrument-footprint width to geomaterial conductivity for uniform homogeneous layers rendered with APhiD. Colored fields from blue to red are imaginary vertical component magnetic field values (B_z^*) expressed in Log_{10} absolute-value form in units of Teslas [T] to bring out the strong gradients at polarity reversals (called "Null Lines" – *Samluk et al.* 2015). Null line nearest to the transmitter (called the "Primary Null Line") defines the cross-sectional size and shape of an EM instrument footprint. Note: footprint varies as a function of conductivity and thickness for different materials and their layering sequence.

Panel (b) shows how the shape and width of the Primary Null Line widens when sea ice of 4.5 meter thickness is introduced in a control run relative to an air-sea interface control run in panel (a). The wider primary null line is consistent over three orders of magnitude for sea ice conductivities for thin ice; around 1 m – not shown for brevity but essentially matching panel (c). But as the sea ice gets thicker, the primary null line begins to vary as a function of sea ice conductivity as well as ice thickness (6-meter case shown in Panel d).

Motivational Field Experiment

Revisiting *McNeill* (1980), we estimate bulk conductivities for sea ice and sea water assuming a three-level system where carry height through air and snow depth are the top known layer with negligible conductivities. Layers two and three are sea ice and sea water, respectively, with unknown bulk conductivities at drill-hole sites where thickness and apparent conductivity are measured directly. Several hundred pairings between instruments at different drill-hole sites form a linear set of equations which subsequently make it possible to estimate the distribution of sea ice and sea water conductivity. Resulting ranges leave us wondering if a constant value is a wise choice for material conductivity of composite geomaterials.

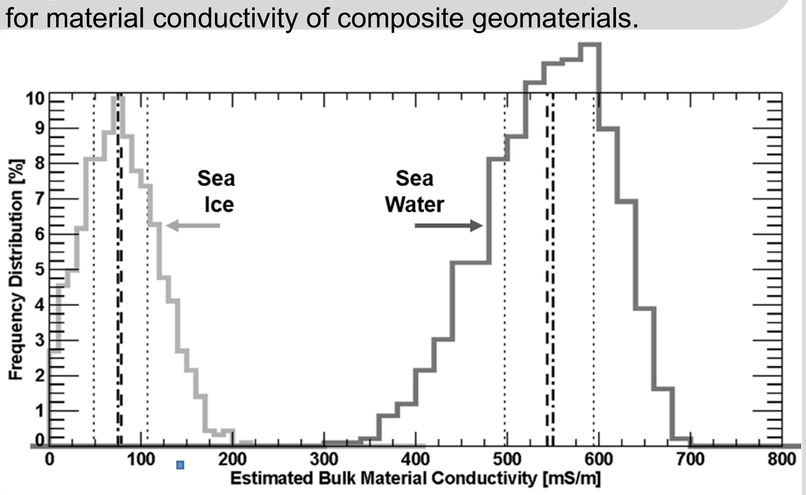

Figure 2. Estimates of bulk conductivity for sea ice and sea water from measurements significantly deviate from traditional assumptions of *homogeneous* half-space layers. Results obtained from coincident EM field measurements made in Barrow Alaska in 2013 at 1 m interval using EM-31 (3.66 m coil separation) and EMP400 (1.25 m coil separation) measurements plus calibration holes every 25 m along a half kilometer transect of relatively flat sea ice (*Woods et al.* 2013, *Samluk* 2016). Central tendencies identified for mean (dashed), median (dot-dash), 25th and 75th percentiles (dotted). Directly sampled in situ material conductivity measurements from Arctic and Antarctic field measurements (e.g., *Sampson et al.* 2011, *Pfaffhuber et al.* 2012) fall within the range of these distributions in support of highly variable, though nearly Gaussian, distribution of local bulk material conductivities for sea ice and sea water.

Motivational Summary

There is a real need to develop new 3-D approaches to understand how non-homogenous geomaterials with variable conductivities interact with induced electromagnetic stationary waves in the kilohertz range.

New Model Visualizations

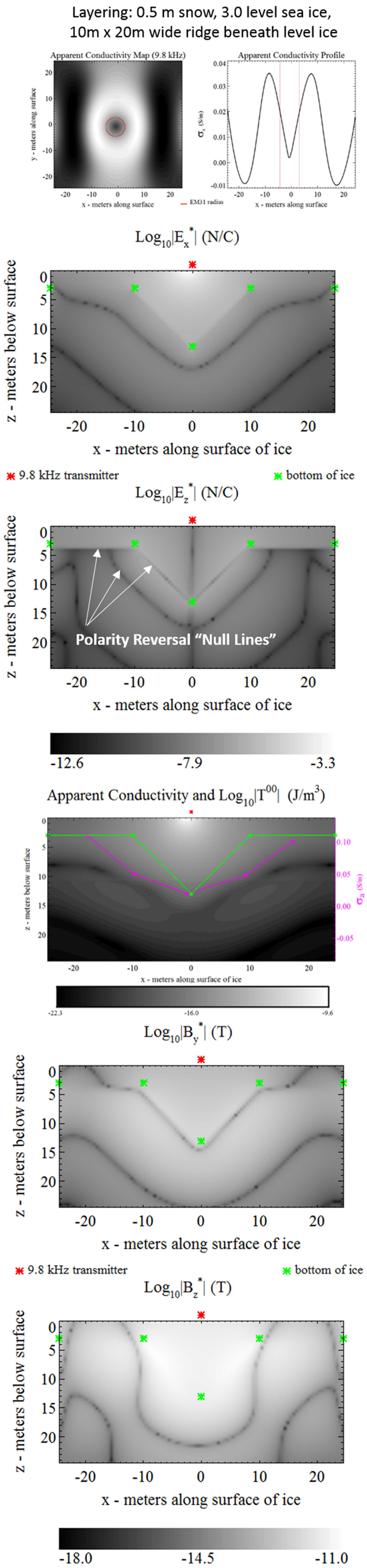

Figure 3. Sample 2-D slices through numerical model results using simulated electromagnetic (EM) induction dipole transmitter (red asterisk) and three layers of potentially wet/dry composite geomaterials. Grey-scale tones used together with log_{10} scaling to communicate EM induction results in a format similar to ground penetrating radar (GPR). Apparent conductivity shown along top panels in three forms: 1) on X-Y plane as a toriod instrument footprint extruded along the Y-axis parallel to the long direction of the ridge, 2) plot of apparent conductivity slice through the X-axis along Y=0, and 3) vertical profile rendering of apparent conductivity (magenta) superimposed on top of Energy Density [J/m3] with ice-water interface delineated in green. Note that the best match between polarity reversals (so called "Null Lines") is not the anticipated vertical imaginary component of the magnetic field (B_z^*), rather it is the vertical imaginary electric field with the horizontally perpendicular components of E_x^* and B_y^* being similar in structure. Note also that the red circle and lines (top left) are not in the peak area where apparent conductivity is strongest. These initial pilot-study results already explain why thicker sea ice is so hard to detect. These new visualizations explain more clearly why larger toroid-shaped instrument footprint corresponds to a conductively weaker geomaterial as one of many points that contradicts 1-D homogeneous earth assumptions in favor of newer 3-D re-examinations of EM induction eddy fields.

New Instrument Design Concepts

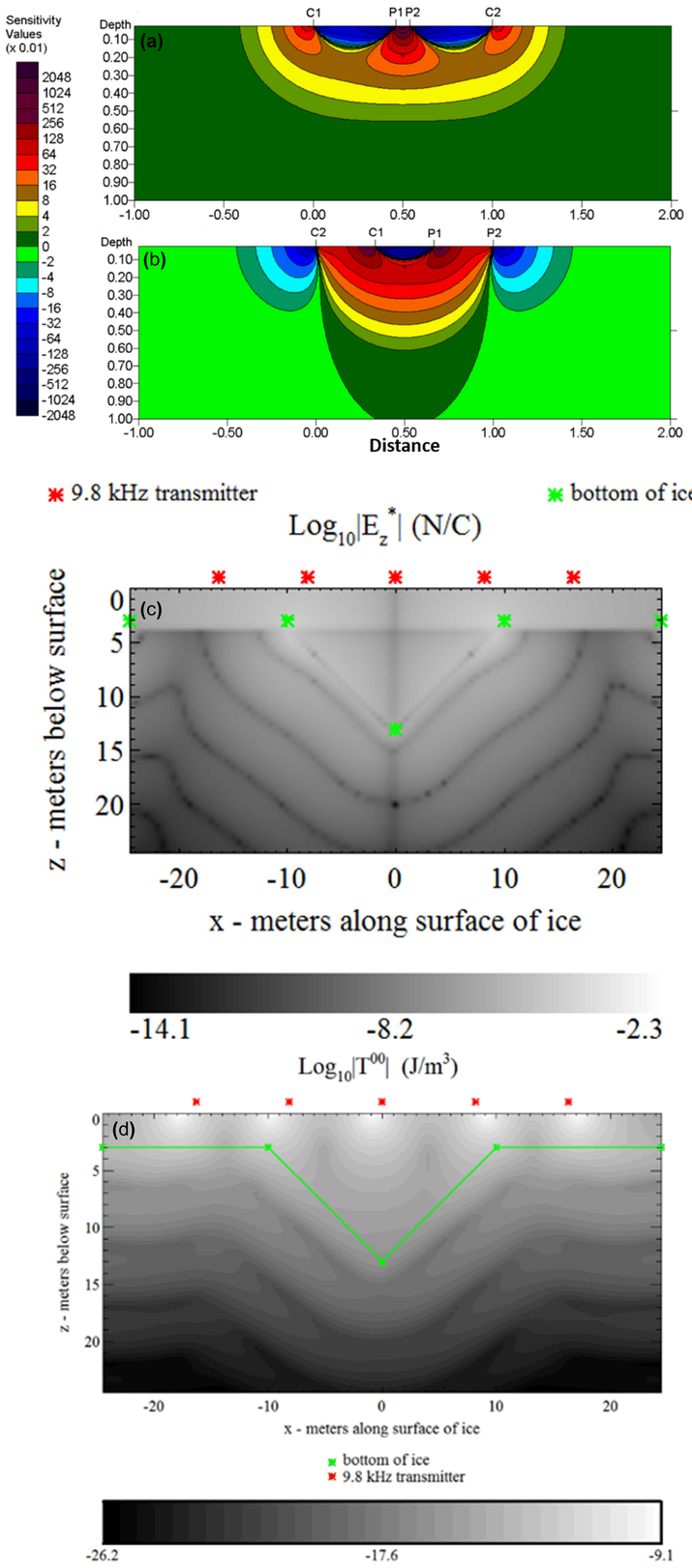

Figure 4. Concept designs for "next generation" instruments. Two different Frechet sensitivity kernels shown for a 4-electrode DC resistivity measurement in the Schlumberger (a) and dipole-dipole (b) configurations over a uniform half-space. Warm colors represent points where a positive conductivity perturbation results in a voltage increase across measurement electrodes P1P2, and cool regions are voltage decrease (adapted from *Loke,* 2010). Panels (c) and (d) show results from the same model as Fig. 3 but with 5 coincident transmitters to demonstrate potential improvements by leveraging resistivity tomography.

Summary/Conclusion To Date

The conductivity of sea ice, being 10% of the sea water, cannot be neglected like air and snow because its smaller conductivity is weighted by its closer proximity to surface transmitters relative to sea water. Hence, greater care and reconsideration of area integration for response functions is warranted. New 3-D models are a positive resource to examine this point more closely and develop new instrumentation which improves the accuracy of non-invasive sea ice thickness estimates.

Related Publications

Geiger, C.A., H.R. Müller, E.R. Bernstein, J.P. Samluk, J.A. Richter-Menge (2015) Impact of spatial aliasing on sea-ice thickness measurements, *Ann. of Glaciol.*, **56**(69), 353-362, doi: 10.3189/2015AoG69A644 http://www.igsoc.org/annals/56/69/.

Loke, M.H. (2010) Tutorial: 2-D and 3-D electrical imaging surveys, http://www.geotomosoft.com

Pfaffhuber AA, Hendricks S, Kvistedal YA (2012) Progressing from 1D to 2D and 3D near-surface airborne electromagnetic mapping with a multisensory, airborne sea-ice explorer. *Geophys.* **77**(4), WB109-WB117.

Samluk J.P. (2016) Investigation of electromagnetic induction retrievals of sea ice thickness using model and measurements, Doctoral Dissertation. University of Delaware, Newark, Delaware, 180 Pp.

Samluk, J.P., C.A. Geiger, and C.J. Weiss (2015) Full-physics 3-D heterogeneous simulations of electromagnetic induction fields on level and deformed sea ice, *Ann. of Glaciol.*, **56**(69), 405-414, doi: 10.3189/2015AoG69A737 http://www.igsoc.org/annals/56/69/.

Sampson, C., K.M. Golden, A. Gully, and A. P. Worby (2011) Surface impedance tomography from Antarctic sea ice, *Deep-Sea Research II,* **58,** 1149-1157, doi:10.1016/j.dsr2.2010.12.003

Weiss, C.J. (2013), Project APhiD: A Lorenz-Gauged **A**-Φ Decomposition for Parallelized Computation of Ultra-Broadband Electromagnetic Induction in a Fully Heterogeneous Earth," *Comput. Geosci.* **58**, 40-52 (2013). http://dx.doi.org/10.1016/j.cageo.2013.05.002i

Woods, J., G. Henderson, **C. A. Geiger,** I. Rigor, T. L. DeLiberty (2013). Spring Break on Ice: U.S. Naval Academy Polar Science Program Field Activities in Barrow, Alaska. Witness the Arctic. 17 (3), 25.